Phase control of light propagation via Fano interference in asymmetric double quantum wells

Wen-Xing Yang, Jia-Wei Lu, Zhi-Kang Zhou, Long Yang, and Ray-Kuang Lee

Citation: Journal of Applied Physics **115**, 203104 (2014); doi: 10.1063/1.4879435
View online: http://dx.doi.org/10.1063/1.4879435
View Table of Contents: http://scitation.aip.org/content/aip/journal/jap/115/20?ver=pdfcov
Published by the AIP Publishing

Phase control of light propagation via Fano interference in asymmetric double quantum wells

Wen-Xing Yang,[1,2,a)] Jia-Wei Lu,[1] Zhi-Kang Zhou,[1] Long Yang,[1] and Ray-Kuang Lee[2]
[1]*Department of Physics, Southeast University, Nanjing 210096, China*
[2]*Institute of Photonics Technologies, National Tsing-Hua University, Hsinchu 300, Taiwan*

(Received 20 April 2014; accepted 13 May 2014; published online 27 May 2014)

We investigate the light propagation and dynamical control of a weak pulsed probe field in asymmetric double quantum wells via Fano interference, which is caused by tunneling from the excited subbands to the same continuum. Our results show that the system can produce anomalous and normal dispersion regions with negligible absorption by choosing appropriate coupling strength of the tunneling and the Fano interference. Interesting enough, the dispersion can be switched between normal and anomalous by adjusting the relative phase between the pulsed probe and coherent control fields owing to the existence of the perfectly Fano interference. Thus, the relative phase can be regarded as a switch to manipulate light propagation with subluminal or superluminal. The temporal and spatial dynamics of the pulsed probe field with hyperbolic secant envelope are analyzed. © *2014 AIP Publishing LLC*. [http://dx.doi.org/10.1063/1.4879435]

I. INTRODUCTION

The study on controlling the group velocity of light propagation and quantum information storage is shown great interest in recent years due to the potential applications in optical communications and quantum information processing.[1–15] The group velocity of a light pulse can be slowed down,[1] or become greater than the speed of light in vacuum or even negative in a special medium.[2,3] Many experimental observations are based on the fact that quantum coherence and interference[16,17] lead to a dispersion profile with a sharp derivative (positive or negative) near the line center.[18] On the other hand, optical transitions between electronic states within the conduction bands of semiconductor quantum wells (SQW) have proved to be a promising candidate for the realization of optical devices and solid quantum information sciences,[19] and large number of efforts has been devoted to the investigations of both quantum coherence and interference in quantum wells.

The development of molecular beam epitaxy (MBE) and band structure engineering has made possible the design and realization of quantum semiconductor structure with new and unusual optical properties. Due to strong electron-electron interactions, the SQWs behave effectively with atomic-like intersubband transition (ISBT) responses.[19] Owing to the small effective electron mass, they have the advantages of high nonlinear optical coefficients and large electric dipole moments of ISBT.[19] Over the past few decades, coherent interaction between electromagnetic fields with ISBT in SQW intrigues, many interesting quantum phenomena[20–29] such as lasing without inversion,[30] slow optical soliton,[31–33] enhancement of four-wave mixing,[34,35] optical switches,[36] and controlling steady-state behaviors.[37–40]

Quantum interference is at the heart of quantum mechanics. Paths interfere when they connect identical initial and final states and the sign of the interference is determined by the phase difference accumulated between the paths. In SQW heterostructures, quantum interference phenomena associated with ISBT optical absorption have been widely demonstrated.[19] In particular, quantum interference arises between absorption paths to two states coupled to a common continuum by tunneling has been observed. This kind of interference is called Fano interference,[19–21] which will lead to nonreciprocal absorptive and dispersive profiles. Recently, we have also studied the slow optical soliton formations based on the Fano interference with a three-level system of electronic subbands in an asymmetric double quantum well (GaAs/AlGaAs) structure, in which the interference between the absorption paths through two resonances to the continuum leads to a linear rapidly varying refractive index change with a reduction in the group velocity.[31] Furthermore, the relative phase of applied laser fields has been widely used for the coherent control of ISBT in QW systems, coined as the phase control technology.[41] Phase control has already been applied for the coherent manipulation of population dynamics and absorption-dispersive properties in QW systems.[42–47]

Motivated by the phase control and Fano-interference, in this paper, we examine the phase controlling the group velocity of light propagating in asymmetric double quantum wells, where two excited states are coupled by tunneling to the same electronic continuum. We reveal that the absorption-dispersive properties and the propagation of pulsed light can be controlled efficiently by adjusting the coupling strength of tunneling and the Fano interference. More interestingly, in presence of the perfect Fano interference, the dispersion can be switched between normal and anomalous by adjusting the relative phase of applied laser fields. This leads to the group velocity of the pulsed probe light switching between subluminal and superluminal. Our results illustrate the potential to utilize relative phase of the coherent fields for controlling group velocity of the light

[a)]Electronic address: wenxingyang2@126.com

pulse in SQW systems, as well as a guidance in the design for possible experimental implementations.

II. THE SYSTEM AND THE DENSITY MATRIX EQUATIONS

We consider the asymmetric SQW structure consisting of two quantum wells that are separated by a narrow barrier as shown in Fig. 1.[31] For a certain bias voltage, the first subband labeled $|a\rangle$ of the shallow well is resonant with the second subband labeled $|b\rangle$ of the deep well (see Fig. 1(a)), and because of the strong coherent coupling via the thin barrier, the levels split into a doublet, i.e., $|2\rangle = (|a\rangle - |b\rangle)/\sqrt{2}$, $|3\rangle = (|a\rangle + |b\rangle)/\sqrt{2}$ (see Fig. 1(b)). The splitting energy ω_s on resonance is given by the coupling strength and can be controlled by adjusting the height and width of the tunneling barrier with applied bias voltage.[31] A low intensity pulsed laser ω_p (amplitude E_p) is applied to the transitions $|1\rangle \rightarrow |2\rangle$ with the respective Rabi frequency $\Omega_p = \mu_{21}E_p/2\hbar$. The transition $|1\rangle \leftrightarrow |3\rangle$ is mediated by coherent control field ω_c (amplitude E_c) with Rabi frequency $\Omega_c = \mu_{31}E_c/2\hbar$. Relevant dipole moments are denoted by μ_{21} and μ_{31}, respectively.

Under the rotating-wave and electro-dipole approximation, in the interaction picture, the semiclassical Hamiltonian describing the system under study can be written as (taking $\hbar = 1$ and the ground state $|1\rangle$ is the energy origin)

$$H_{\text{int}}^{I} = -\Delta_p|2\rangle\langle 2| - \Delta_c|3\rangle\langle 3| + \Omega_p e^{i\phi_p}|2\rangle\langle 1| + \Omega_c e^{i\phi_c}|3\rangle\langle 1| + H.c., \quad (1)$$

where $\Delta_p = \omega_p - \omega_{21}$ and $\Delta_c = \omega_c - \omega_{31}$ are the detunings of probe field and coherent control fields, respectively, and ω_{j1} $(j = 2, 3)$ is the corresponding transition frequency. $\phi_{p,c}$ is the phase of the corresponding fields. Using the Weisskopf-Wigner theory, we can obtain the density matrix equations for this system

$$i\frac{\partial \rho_{22}}{\partial t} = \Omega_p\rho_{12} - \Omega_p^*\rho_{21} - i\gamma_2\rho_{22} - \frac{i}{2}\eta(\rho_{23} + \rho_{32}), \quad (2)$$

$$i\frac{\partial \rho_{33}}{\partial t} = \Omega_c e^{i\phi}\rho_{13} - \Omega_c^* e^{-i\phi}\rho_{31} - i\gamma_3\rho_{33} - \frac{i}{2}\eta(\rho_{23} + \rho_{32}), \quad (3)$$

$$i\frac{\partial \rho_{12}}{\partial t} = \Omega_p^*(\rho_{22} - \rho_{11}) + \Omega_c^*\rho_{32} + \Delta_p\rho_{12} - \frac{i}{2}\gamma_{21}\rho_{12} - \frac{i}{2}\eta\rho_{13}, \quad (4)$$

$$i\frac{\partial \rho_{13}}{\partial t} = \Omega_c^* e^{-i\phi}(\rho_{33} - \rho_{11}) + \Omega_p^*\rho_{23} + \Delta_c\rho_{13} - \frac{i}{2}\gamma_{31}\rho_{13} - \frac{i}{2}\eta\rho_{12}, \quad (5)$$

$$i\frac{\partial \rho_{23}}{\partial t} = -\Omega_c^* e^{-i\phi}\rho_{21} + \Omega_p\rho_{13} + (\Delta_c - \Delta_p)\rho_{23} + \omega_s\rho_{23} - \frac{i}{2}\gamma_{32}\rho_{23} - \frac{i}{2}\eta(\rho_{22} + \rho_{33}), \quad (6)$$

together with $\rho_{11} + \rho_{22} + \rho_{33} = 1$ and $\rho_{ij} = \rho_{ji}^*$. $\omega_s = \omega_{31} - \omega_{21}$ is the energy splitting between the upper levels $|2\rangle$ and $|3\rangle$. The parameter $\phi = \phi_c - \phi_p$ is the relative phase between the two fields. The population decay rates and the dephasing rates are added phenomenologically in the above equations. The population decay rates for subband $|j\rangle$ $(j = 1, 2, 3)$, denoted by γ_j, are due primarily to longitudinal optical (LO) phonon emission events at low temperature. The total decay rates γ_{ij} $(i \neq j)$ are given by $\gamma_{21} = \gamma_2 + \gamma_{21}^{dph}$, $\gamma_{31} = \gamma_3 + \gamma_{31}^{deph}$, and $\gamma_{32} = \gamma_2 + \gamma_3 + \gamma_{32}^{dph}$, where γ_{ij}^{dph}, determined by carrier-carrier scattering, interface roughness, and phonon scattering processes, is the dephasing decay rates of quantum coherence of the $|i\rangle \leftrightarrow |j\rangle$ transitions. The population decay rates can be calculated by solving the effective mass Schrödinger equation. And as we know, the initially nonthermal carrier distribution is quickly broadened due to inelastic carrier-carrier scattering, with the broadening rate increasing as carrier density is increased. For the temperatures up to 10 K, the carrier density smaller than $10^{12}\,\text{cm}^{-2}$, the dephasing decay rates γ_{ij}^{dph} can be estimated according to Refs. 31–36. For the present SQW system, they turn out to be $\gamma_2 = 5.6\,\text{meV}$, $\gamma_3 = 7\,\text{meV}$, $\gamma_{21} = 1.5\,\text{meV}$, $\gamma_{31} = 2.3\,\text{meV}$, and $\gamma_{32} = 1.9\,\text{meV}$. $\eta = p\sqrt{\gamma_2\gamma_3}$ denotes a cross coupling term between the excited states $|2\rangle$ and $|3\rangle$, due to the Fano-type interference in the electronic continuum. It is noted that p represents the strength of Fano-type interference, where the values $p = 0$ and $p = 1$ correspond to no interference and perfect interference, respectively.[19–21]

III. NUMERICAL ANALYSIS FOR CONTROLLING THE GROUP VELOCITY

In this section, we will study manipulating the group velocity of the weak probe laser ω_p. The group velocity is defined by $v_g = c/n_g$, where n_g and c are the group refractive

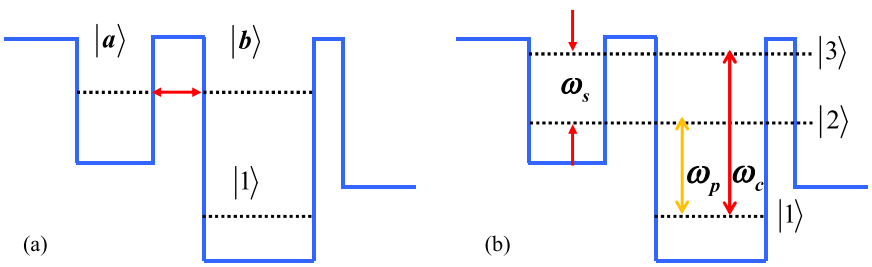

FIG. 1. Schematic band diagram of the asymmetric double quantum wells. (a) Subband $|a\rangle$ of the shallow well is resonant with the second subband $|b\rangle$ of the deep well. (b) Due to the strong coherent coupling via the thin barrier, the subbands split into a doublet $|2\rangle$ and $|3\rangle$, which are coupled to a continuum by a thin tunneling barrier adjacent to the deep well. ω_s is the energy splitting between the upper levels $|2\rangle$ and $|3\rangle$ (the coupling strength of tunneling), ω_p and ω_c are the frequencies of the corresponding probe and control laser fields, respectively.

index and vacuum light speed, respectively. The group refractive index n_g is related to the susceptibility χ_{21} for the corresponding transition $|1\rangle \leftrightarrow |2\rangle$

$$n_g = 1 + \frac{1}{2}\mathrm{Re}[\chi_{21}] + \frac{1}{2}\omega_p \frac{\partial \mathrm{Re}[\chi_{21}]}{\partial \omega_p}, \tag{7}$$

together with $\chi_{21} = \frac{2N|\mu_{21}|^2}{\hbar\varepsilon_0\Omega_p}\rho_{21}(t)$, where N is the electron density in the conduction band of quantum well and ε_0 is the vacuum dielectric constant. $\mathrm{Re}[\chi_{21}]$ represents the real part of the susceptibility χ_{21}. Here, our main interest is the absorption-dispersion properties of the probe laser, from which we can simply demonstrate the possible effects of the relative phase, the control fields and the Fano-type interference on the group velocity. If the dispersion curve is normal and the absorption is negligible, the group velocity will be significantly reduced and the subluminal phenomenon exhibits. On the other hand, if the dispersion is anomalous and the absorption can be neglected, the group velocity will be increased or even becomes negative and the superluminal phenomenon exhibits. In the limit of a weak probe, the absorption-dispersion coefficients for the probe laser are governed by the real and imaginary parts of the susceptibility, i.e., $\chi_{21} \propto \rho_{21}(t)$. In the following, we will directly examine the transient absorption-dispersion property of the weak probe laser by numerically integrating Eqs. (2)–(6) with a certain initial condition. With the initial conditions $\rho_{11}(0) = 1$, $\rho_{22,33}(0) = 0$, and $\rho_{ij}(0) = 0$ for $i \neq j$ ($i, j = 1, 2, 3$), we solve the time-dependent Eqs. (2)–(6) by a standard fourth-order Runge-Kutta method. Note that, the Rabi frequencies Ω_p and Ω_c are assumed to be real constants in our numerical simulations.

We first analyze the influences of the tunneling coupling on the absorption-dispersion curves of the probe laser with including the perfect Fano interference in this SQW system. Here, the frequency detuning of the control field, the strength of Fano interference, the relative phase between the probe and control field, and the intensities of the probe and control fields are $\Delta_c = 0$, $p = 0.9$, $\phi = 0$, $\Omega_p = 0.01$ meV, and $\Omega_c = 8$ meV. We plot in Fig. 2, the real and imaginary parts of ρ_{21} as a function of the detuning Δ_p for different values of ω_s, i.e., $\omega_s = 20$ meV (Fig. 2(a)) and $\omega_s = 35$ meV (Fig. 2(b)). From Fig. 2, one can find that the absorption-dispersion curves depend significantly on the coupling strength of tunneling ω_s. Fig. 2(a) shows that a negative steep dispersion curve can be observed and it is accompanied by a wide transparency window around probing resonance (i.e., $\Delta_p = 0$) between two absorption lines. According to Eq. (7), the negative dispersion curve corresponds to a anomalous dispersion and leads to increasing of the group velocity of the probe laser. Contrarily, Fig. 2(b) illustrates that the normal dispersion accompanied by transparency at $\Delta_p = 0$ between two gain lines can be observed in the absorption-dispersion curve, which implies that slowing down of the corresponding group velocity occurs. In other words, the group velocity of the probe laser propagating through the SQW structure can be manipulated from superluminal to subluminal by adjusting the coupling strength of tunneling ω_s. It should be noted that the coupling strength of tunneling can be controlled by adjusting the height and width of the tunneling barrier. Therefore, the group velocity of the probe laser can be switched between superluminal and subluminal by tuned the tunneling barrier. And this optical switching provides an efficient and convenient way to achieve slow- and fast-light.

Second, we analyze the influences of the strength or quality of the Fano interference on the dispersion-absorption curves of the probe laser with a certain coupling strength of tunneling (i.e., $\omega_s = 20$ meV) in the present SQW system. As shown in Fig. 3, we plot the real and imaginary parts of ρ_{21} as a function of the detuning Δ_p for different values of p, i.e., $p = 0.4$ (Fig. 3(a)) and $p = 0.8$ (Fig. 3(b)). As can be seen from Fig. 3, the absorption-dispersion curves depend sensitively on the value of parameter p. In the case of $p = 0.4$, a small absorption peak around the probing resonance position ($\Delta_p = 0$) can be observed in the absorption curve. At the same time, the dispersion curve exhibits steep and positive slope, which means subluminal propagation of the probe field occurs. On the other hand, in the case of $p = 0.8$, the curves of Fig. 3(b) exhibit a negative slope accompanied by negligible absorption around $\Delta_p = 0$, which corresponds to superluminal propagation of the probe field. Different from the scheme for controlling group velocity in atom system,[1–15] the parameters of the electron subbands in SQW structures can be engineered to give a desired strength of interference by utilizing so-called structure coherent control in design.[19] Thus, we may provide a novel method to

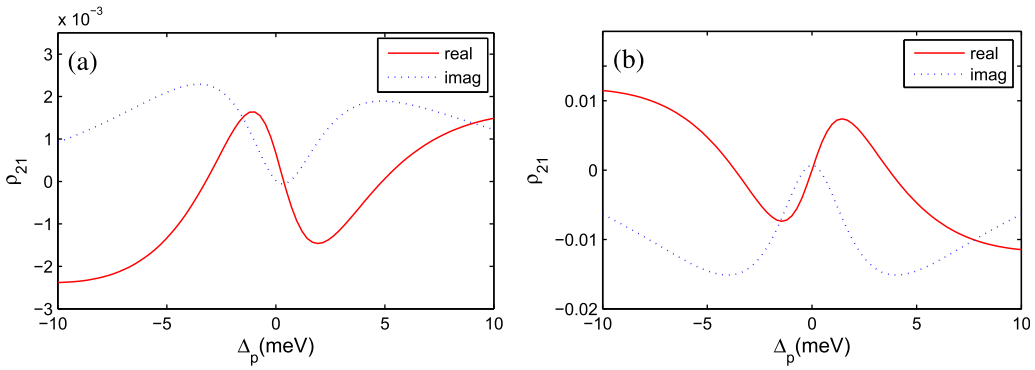

FIG. 2. The real (solid line) and imaginary (dotted line) parts of ρ_{21} as a function of the detuning of the probe field Δ_p with different coupling strengths of the tunneling (a) $\omega_s = 20$ meV and (b) $\omega_s = 35$ meV. The other values of the parameters are chosen as $\phi = 0$, $\Delta_c = 0$, $\gamma_2 = 5.6$ meV, $\gamma_3 = 7$ meV, $\gamma_{21} = 1.5$ meV, $\gamma_{31} = 2.3$ meV, $\gamma_{32} = 1.9$ meV, $p = 0.9$, $\Omega_c = 8$ meV, and $\Omega_p = 0.01$ meV.

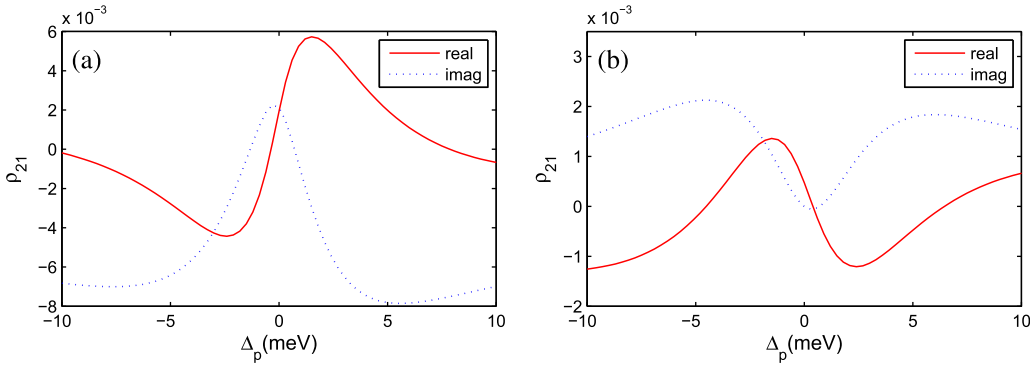

FIG. 3. The real (solid line) and imaginary (dotted line) parts of ρ_{21} as a function of the detuning of the probe field Δ_p with different strengths of the Fano interference (a) $p = 0.4$ and (b) $p = 0.8$. The other values of the parameters are chosen as $\phi = 0$, $\Delta_c = 0$, $\gamma_2 = 5.6$ meV, $\gamma_3 = 7$ meV, $\gamma_{21} = 1.5$ meV, $\gamma_{31} = 2.3$ meV, $\gamma_{32} = 1.9$ meV, $\Omega_c = 8$ meV, $\omega_s = 20$ meV, and $\Omega_p = 0.01$ meV.

manipulate the group velocity and the absorption of the probe filed in solid-state system.

Up to now, we have investigated controlling the absorption-dispersion curves and manipulating the group velocity of the probe laser via varying the coupling strength of tunneling and Fano interference. We now examine the effect of the relative phase ϕ between the control and probe fields on the absorption-dispersion curves. We should note that the relative phase of applied laser fields has been widely used for the coherent control of ISBT in SQW systems, coined as the phase control technology.[19,42–47] In the absence of the Fano interference (i.e., $p = 0$), we plot in Figs. 4(a) and 4(b), the real and imaginary parts of ρ_{21} versus Δ_p with different values of ϕ, i.e., $\phi = 0$ (see Fig. 4(a)) and $\phi = \pi$ (see Fig. 4(b)). It is shown that the same positive and steep dispersion with a small absorption peak at probing resonance can be observed both in Figs. 4(a) and 4(b), which means that the subluminal propagation of the probe field occurs in this SQW system. That is, the influences of the relative phase ϕ on the dispersion curves can be ignored when the Fano interference is not included. As a result, in this case, we cannot change the group velocity of the probe laser from subluminal to superluminal or vice versa by varying the relative phase ϕ. In presence of the perfect Fano interference (i.e., $p = 0.9$), we show in Figs. 4(c) and 4(d), the real and imaginary parts of ρ_{21} versus Δ_p. From Fig. 4(c), one can easily observe a negative and steep dispersion curve accompanied with transparency at probing resonant position $\Delta_p = 0$, which presents the anomalous dispersion. Thus, the superluminal propagation of the probe laser can be achieved, in this case. Interestingly enough, if the relative phase ϕ is switched into π, Fig. 4(d) illustrates that the slope of dispersion curve

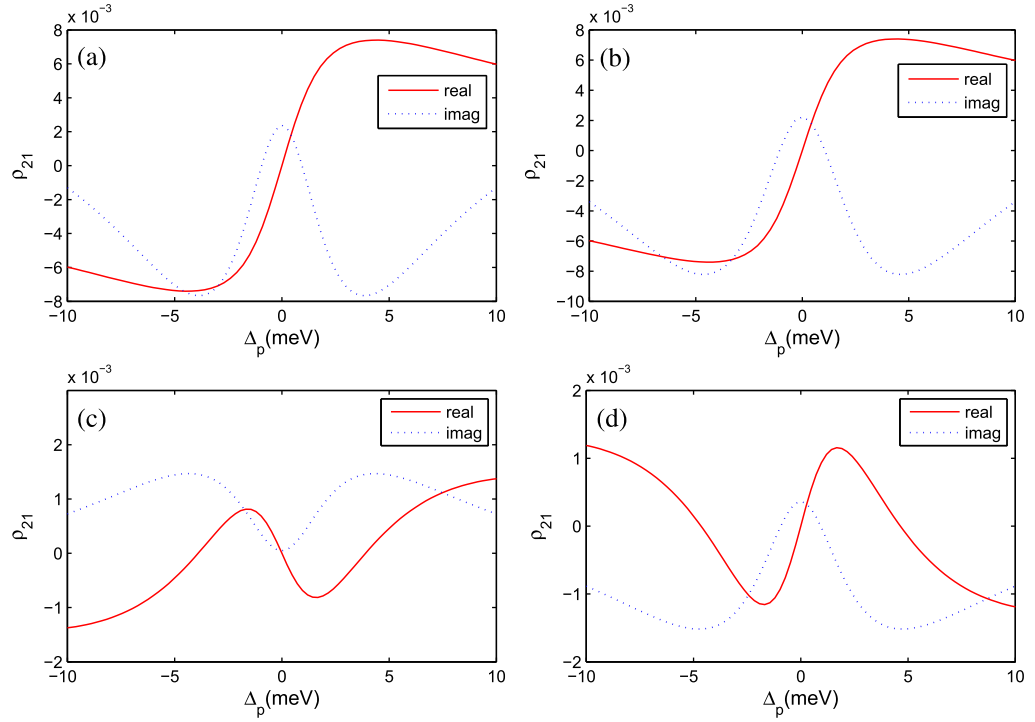

FIG. 4. The real (solid line) and imaginary (dotted line) parts of ρ_{21} as a function of the detuning of the probe field Δ_p with different cases (a) $\phi = 0$, $p = 0$; (b) $\phi = \pi$, $p = 0$; (c) $\phi = 0$, $p = 0.9$; and (d) $\phi = \pi$, $p = 0.9$. The other values of the parameters are chosen as $\Delta_c = 0$, $\gamma_2 = 5.6$ meV, $\gamma_3 = 7$ meV, $\gamma_{21} = 1.5$ meV, $\gamma_{31} = 2.3$ meV, $\gamma_{32} = 1.9$ meV, $\Omega_c = 8$ meV, $\omega_s = 20$ meV, and $\Omega_p = 0.01$ meV.

becomes into positive but the absorption shows to be enlarged slightly at $\Delta_p = 0$. That is, subluminal propagation of the probe laser can be observed, in this case. Thus, one can easily conclude the Fano interference plays an important role in controlling the absorption-dispersion properties of the probe laser in the present SQW system. Furthermore, due to the existence of the perfect Fano interference, one can efficiently control the dispersion curve of the probe laser and corresponding group velocity can be switched between superluminal and subluminal by simply adjusting the relative phase ϕ between the applied laser fields.

For a directly insight into the modulation of the relative phase between the probe and control fields on the group velocity of probe laser in the present SQW system, we now numerically simulated the group index n_g versus the relative phase ϕ. The present asymmetric double SQW structure (GaAs/AlGaAs) has been studied in several previous works.[19–21,31] For temperature up to 10 K, the value of electron sheet density is about $N = 10^{12}\,\mathrm{cm}^{-2}$. The small value of N ensures that the system is initially in the lowest state $|1\rangle$, so that the initial conditions can be satisfied in our numerical simulations (i.e., $\rho_{11}(0) = 1$, $\rho_{22,33}(0) = 0$). The dipole matrix element can be given $\mu_{21} = e \times 4.2\,\mathrm{nm}$. Under the condition of probing resonance, we choose $\omega_p = \omega_{12} = 120\,\mathrm{meV}$ In Fig. 5, we present the dependence of group index n_g on the relative phase ϕ for different coupling strengths of the tunneling ω_s and Fano interference p. The curves of Fig. 5 illustrate that the group index has a significant dependence on the relative phase between the probe and control fields in presence of the perfect Fano interference (i.e., $p \neq 0$). As shown in Fig. 5(a), the curves of group index oscillate between positive values and negative values periodically as the relative phase changes, which mean that the group velocity of probe laser can be switched between subluminal and superluminal periodically. In addition, Fig. 5(a) also clearly illustrates that oscillating amplitude of the phase-dependent group index can be decreased as the coupling strength of tunneling increases. These results might be useful to control the group velocity of the probe laser simply by adjusting the splitting between the two excited states. Besides, it can be seen from Fig. 5(b), the perfect Fano interference induces large phase modulation of the group index, which can be well explained using the perturbation theory. It should be noted that Eqs. (2)–(6) characterize the density-matrix element ρ_{21} having the period 2π for the relative phase ϕ, Eq. (7) implies that the group index n_g should approximately have the period 2π for the phase ϕ, just as clearly shown in Fig. 5.

IV. THE TEMPORAL AND SPATIAL DYNAMICS OF THE PROBE PULSE

As discussed above, we have investigated how to manipulate the dispersion property and group velocity of the probe laser by adjusting appropriately parameters of the present SQW system. As illustrated in Figs. 2–5, except for rare cases (i.e., the large coupling strength of tunneling $\omega_s = 35\,\mathrm{meV}$ and without including the Fano interference $p = 0$), all cases of superluminal or subluminal behavior considered here are accompanied by a negligible absorption or gain under the condition of probing resonance. If the absorption or gain cannot be neglected, we should consider explicitly the propagation dynamic of a well defined wave-packet to show whether or not it can propagate without distortions according to the calculated group velocity. Therefore, in this section, we will examine the temporal and spatial dynamics of probe laser propagating in this SQW system under the condition that a significant loss or gain effect is accompanied. This is a rather relevant issue, which has remained open both theoretically and experimentally. Under the slowly varying-envelope approximation, the propagating dynamics of the probe laser pulse is described by the Maxwell equation along the propagating direction z direction[31–34]

$$\frac{\partial \Omega_p(z,t)}{\partial z} + \frac{1}{c}\frac{\partial \Omega_p(z,t)}{\partial t} = i\kappa\rho_{21}(t), \tag{8}$$

where $\kappa_{21} = N\Omega_p|\mu_{12}|^2/(2\varepsilon_0\hbar c)$. For simplicity of the analysis, we take $\Omega_p(z,t) = \Omega_p f(z,t)$ with Ω_p the real constant describing the maximal value of Rabi frequency and $f(z, t)$ a dimensionless spatiotemporal pulse envelope function, respectively. In the local (retarded) frame, where $\xi = z$ and $\eta = t - z/c$, the propagation of the probe laser pulse across the present SQW system can be described by the motion equations for density matrix elements $\rho_{ij}(\xi, \eta)$ and the normalized pulse envelope $f(\xi, \eta)$ as

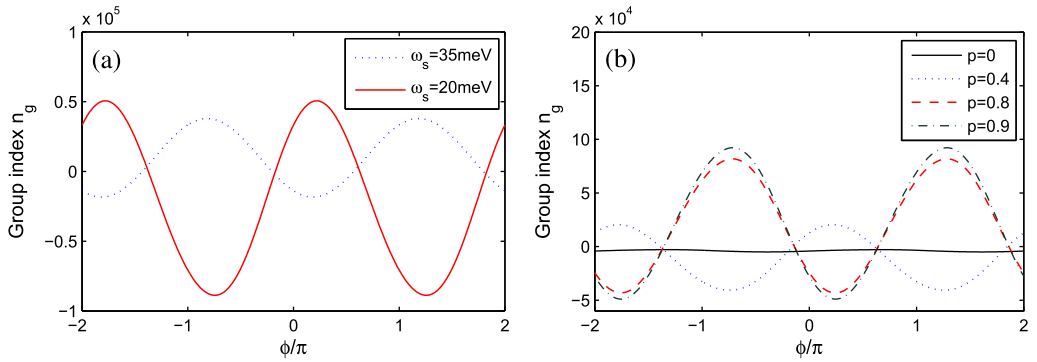

FIG. 5. The group index n_g as a function of the relative phase ϕ (a) with $p = 0.9$ and different coupling strengths of the tunneling $\omega_s = 20\,\mathrm{meV}$ (solid line) and $\omega_s = 35\,\mathrm{meV}$ (dotted line); (b) with $\omega_s = 20\,\mathrm{meV}$ and different strengths of the Fano interference $p = 0$ (solid line), $p = 0.4$ (dotted line), $p = 0.8$ (dashed line), and $p = 0.9$ (dashed-dotted line). The other values of the parameters are chosen as $\Delta_c = 0$, $\gamma_2 = 5.6\,\mathrm{meV}$, $\gamma_3 = 7\,\mathrm{meV}$, $\gamma_{21} = 1.5\,\mathrm{meV}$, $\gamma_{31} = 2.3\,\mathrm{meV}$, $\gamma_{32} = 1.9\,\mathrm{meV}$, $\Omega_c = 8\,\mathrm{meV}$, and $\Omega_p = 0.01\,\mathrm{meV}$.

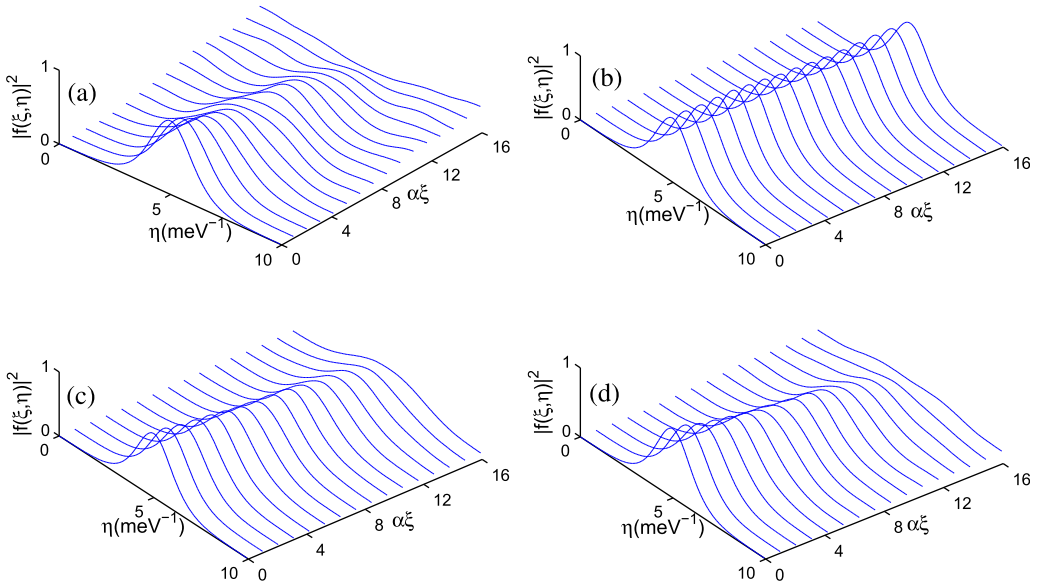

FIG. 6. The temporal and spatial evolution of the magnitude squared of the pulse envelopes: (a) with $p=0$ and (b) $p=0.9$ for $\phi=0$ and $\omega_s=20$ meV; (c) with $\phi=\pi$, $p=0.9$, and $\omega_s=20$ meV; and (d) with $\phi=0$, $p=0.9$, and $\omega_s=35$ meV. The other values of the parameters are chosen as $\Delta_c=0$, $\gamma_2=5.6$ meV, $\gamma_3=7$ meV, $\gamma_{21}=1.5$ meV, $\gamma_{31}=2.3$ meV, $\gamma_{32}=1.9$ meV, $\Omega_c=8$ meV, and $\Omega_p=0.01$ meV.

$$i\frac{\partial\rho_{22}(\xi,\eta)}{\partial\eta}=\Omega_p f(\xi,\eta)\rho_{12}(\xi,\eta)-\Omega_p f^*(\xi,\eta)\rho_{21}(\xi,\eta) -i\gamma_2\rho_{22}(\xi,\eta)-\frac{i}{2}\eta(\rho_{23}(\xi,\eta)+\rho_{32}(\xi,\eta)), \quad (9)$$

$$i\frac{\partial\rho_{33}(\xi,\eta)}{\partial\eta}=\Omega_c e^{i\phi}\rho_{13}(\xi,\eta)-\Omega_c^* e^{-i\phi}\rho_{31}(\xi,\eta) -i\gamma_3\rho_{33}(\xi,\eta)-\frac{i}{2}\eta(\rho_{23}(\xi,\eta)+\rho_{32}(\xi,\eta)), \quad (10)$$

$$i\frac{\partial\rho_{12}(\xi,\eta)}{\partial\eta}=\Omega_p f^*(\xi,\eta)(\rho_{22}(\xi,\eta)-\rho_{11}(\xi,\eta)) +\Omega_c^*\rho_{32}(\xi,\eta)+\Delta_p\rho_{12}(\xi,\eta) -\frac{i}{2}\gamma_{21}\rho_{12}(\xi,\eta)-\frac{i}{2}\eta\rho_{13}(\xi,\eta), \quad (11)$$

$$i\frac{\partial\rho_{13}(\xi,\eta)}{\partial\eta}=\Omega_c^* e^{-i\phi}(\rho_{33}(\xi,\eta)-\rho_{11}(\xi,\eta)) +\Omega_p f^*(\xi,\eta)\rho_{23}(\xi,\eta)+\Delta_c\rho_{13}(\xi,\eta) -\frac{i}{2}\gamma_{31}\rho_{13}(\xi,\eta)-\frac{i}{2}\eta\rho_{12}(\xi,\eta), \quad (12)$$

$$i\frac{\partial\rho_{23}(\xi,\eta)}{\partial\eta}=-\Omega_c^* e^{-i\phi}\rho_{21}(\xi,\eta)+\Omega_p\rho_{13}(\xi,\eta) +(\Delta_c-\Delta_p)\rho_{23}(\xi,\eta)+\omega_s\rho_{23}(\xi,\eta) -\frac{i}{2}\gamma_{32}\rho_{23}(\xi,\eta)-\frac{i}{2}\eta(\rho_{22}(\xi,\eta) +\rho_{33}(\xi,\eta)), \quad (13)$$

$$i\frac{\partial f(\xi,\eta)}{\partial\alpha\xi}=\frac{\gamma_{21}}{\Omega_p f(\xi,\eta)}\rho_{21}(\xi,\eta), \quad (14)$$

where the propagation constant on the left-hand side of the above equation is given by $\alpha=N\omega_p|\mu_{21}|^2/4\hbar\varepsilon_0 c\gamma_{21}$. Now, we numerically solve Eqs. (9)–(14) with the initial condition that all the electrons start in the ground state $|1\rangle$ and the boundary condition that the pulsed probe laser is assumed as a hyperbolic secant pulse at the beginning of the SQW system $\xi=0$ ($f(0,\ \eta)=\mathrm{sech}(\pi\eta/\tau_p)$). In Fig. 6, we show the result of numerical simulation on the hyperbolic secant wave shape $|f(\xi,\eta)|^2$ with pulse duration $\tau_p=10$ meV (-1) versus the time η and distance $\alpha\xi$. It can be found from Fig. 6(a) that the probe absorption increases significant as the propagation distance increases, and the probe laser is completely absorbed over the lengths shorter than $16/\alpha$ when the Fano interference does not exist. From Fig. 6(b), in presence of the perfect Fano interference, we can see that the probe pulse can propagate with appreciable transparent even through a sufficiently long distances. The corresponding group velocity of the probe field can be calculated as $v_g=c/n_g=-9.4\times10^3$ m/s. When keeping all other parameters fixed but changing the relative phase ϕ from 0 to π, Fig. 6(c) illustrates that the absorption of the probe laser increases slightly with propagation. Accordingly, the group velocity of the probe laser $v_g=c/n_g=6.1\times10^3$ m/s. Fig. 6(d) clearly shows that, when the coupling strength of tunneling ω_s increases, the corresponding absorption can also increase and the distortion of the pulse propagation becomes obviously. Thus, owing to the high-quality Fano interference, the group velocity of the pulse propagation can be switched from superluminal to subluminal or vice versa via adjusting the relative phase between the probe and control fields. It is worth noting that the pulse distortion will appear as the propagation distance increases. However, the distortion-free propagation of the probe pulse can be also realized when the nonlinear effects of the system are included.[31–34]

V. CONCLUSION

In conclusion, we have investigated the absorption-dispersion property and the propagating dynamics of a weak probe laser based on the ISBT in asymmetric double

quantum wells via Fano interference, which is caused by tunneling from the excited subbands to the same continuum. By solving the density matrix equations of the motion numerically, our results show that coupling strength of the tunneling and the Fano interference can significantly modify the optical properties of the double SQW structure. As a result, by choosing appropriately these parameters, the group index of the probe laser can be manipulated efficiently and both the subluminal and superluminal light propagations can be observed. More interestingly, if high-quality Fano interference is presence, can be switched between normal and anomalous by adjusting the relative phase between the pulsed probe and coherent control fields. In other words, the group velocity of light propagation can be switched between subluminal and superluminal simply by changing this relative phase. Our calculations provide a guideline for optimizing and controlling the optical switching of the group velocity in the SQW solid-state system, which is much more practical than that in atomic system because of its flexible design and the controllable interference strength.

ACKNOWLEDGMENTS

The research was supported in part by National Natural Science Foundation of China under Grant Nos. 11374050 and 61372102, by Qing Lan project of Jiangsu, and by the Fundamental Research Funds for the Central Universities under Grant No. 2242012R30011.

[1]L. V. Hau, S. E. Harris, Z. Dutton, and C. H. Behroozi, Nature (London) **397**, 594 (1999).
[2]L. J. Wang, A. Kuzmich, and A. Dogariu, Nature (London) **406**, 277 (2000).
[3]A. M. Steinberg and R. Y. Chiao, Phys. Rev. A **49**, 2071 (1994).
[4]M. S. Bigelow, N. N. Lepeshkin, and R. W. Boyd, Science **301**, 200 (2003).
[5]M. S. Bigelow, N. N. Lepeshkin, and R. W. Boyd, Phys. Rev. Lett. **90**, 113903 (2003).
[6]M. O. Scully, Nature (London) **426**, 610 (2003).
[7]M. O. Scully and M. S. Zubairy, Science **301**, 181 (2003).
[8]Y. Wu, M. G. Payne, E. W. Hagley, and L. Deng, Phys. Rev. A **69**, 063803 (2004).
[9]Y. Wu, M. G. Payne, E. W. Hagley, and L. Deng, Phys. Rev. A **70**, 063812 (2004).
[10]D. F. Phillips, A. Fleischhauer, A. Mair, R. L. Walsworth, and M. D. Lukin, Phys. Rev. Lett. **86**, 783 (2001).
[11]M. Bajcsy, A. S. Zibrov, and M. D. Lukin, Nature (London) **426**, 638 (2003).
[12]Y. Wu and X. Yang, Phys. Rev. A **70**, 053818 (2004).
[13]A. Dogariu, A. Kuzmich, and L. J. Wang, Phys. Rev. A **63**, 053806 (2001).
[14]D. Han, Y. Zeng, Y. Bai, H. Cao, W. Chen, C. Huang, and H. Lu, Opt. Commun. **281**, 4712 (2008).
[15]D. Han, Y. Zeng, and Y. Bai, Opt. Commun. **284**, 4541 (2011).
[16]Y. Wu, M. G. Payne, E. W. Hagley, and L. Deng, Opt. Lett. **29**, 2294 (2004).
[17]Y. Wu and L. Deng, Opt. Lett. **29**, 1144 (2004).
[18]S. E. Harris, Phys. Today **50**(7), 36 (1997).
[19]H. C. Liu and F. Capasso, *Intersubband Transitions in Quantum Wells: Physics and Device Applications* (Academic, New York, 2000).
[20]J. Faist, F. Capasso, C. Sirtori, K. W. West, and L. N. Pfeiffer, Nature **390**, 589 (1997).
[21]H. Schmidt, K. L. Campman, A. C. Gossard, and A. Imamoglu, Appl. Phys. Lett. **70**, 3455 (1997).
[22]G. B. Serapiglia, E. Paspalakis, C. Sirtori, K. L. Vodopyanov, and C. C. Phillips, Phys. Rev. Lett. **84**, 1019 (2000).
[23]H. Choi, V. M. Gkortsas, L. Diehl, D. Bour, S. Corzine, J. Zhu, G. Höfler, F. Capasso, F. X. Kärtner, and T. B. Norris, Nature Photon. **4**, 706 (2010).
[24]T. Müller, W. Parz, G. Strasser, and K. Unterrainer, Phys. Rev. B **70**, 155324 (2004).
[25]J. F. Dynes, M. D. Frogley, M. Beck, J. Faist, and C. C. Phillips, Phys. Rev. Lett. **94**, 157403 (2005).
[26]M. Wagner, H. Schneider, D. Stehr, S. Winnerl, A. M. Andrews, S. Schartner, G. Strasser, and M. Helm, Phys. Rev. Lett. **105**, 167401 (2010).
[27]S. G. Kosionis, A. F. Terzis, and E. Paspalakis, J. Appl. Phys. **109**, 084312 (2011).
[28]E. Paspalakis, C. Simserides, and A. Terzis, J. Appl. Phys. **107**, 064306 (2010).
[29]S. G. Kosionis, A. Terzis, C. Simserides, and E. Paspalakis, J. Appl. Phys. **108**, 034316 (2010).
[30]M. D. Frogley, J. F. Dynes, M. Beck, J. Faist, and C. C. Phillips, Nature Mater. **5**, 175 (2006).
[31]W. X. Yang, J. M. Hou, and R. K. Lee, Phys. Rev. A **77**, 033838 (2008).
[32]W. X. Yang, J. M. Hou, Y. Y. Lin, and R. K. Lee, Phys. Rev. A **79**, 033825 (2009).
[33]W. X. Yang, A. X. Chen, R. K. Lee, and Y. Wu, Phys. Rev. A **84**, 013835 (2011).
[34]W. X. Yang, J. M. Hou, and R. K. Lee, J. Mod. Opt. **56**, 716 (2009).
[35]H. Sun, S. Fan, H. Zhang, and S. Gong, Phys. Rev. B **87**, 235310 (2013).
[36]J. H. Wu, J. Y. Gao, J. H. Xu, L. Silvestri, M. Artoni, G. C. LaRocca, and F. Bassani, Phys. Rev. Lett. **95**, 057401 (2005).
[37]A. Joshi and M. Xiao, Appl. Phys. B: Lasers Opt. **79**, 65 (2004).
[38]J. H. Li, X. Hao, J. Liu, and X. Yang, Phys. Lett. A **372**, 716 (2008).
[39]Z. Wang and B. Yu, J. Appl. Phys. **113**, 113101 (2013).
[40]N. Heidari and M. Mahmoudi, Physica E **44**, 1288 (2012).
[41]M. Shapiro and P. Brumer, Rep. Prog. Phys. **66**, 859 (2003).
[42]J. F. Dynes and E. Paspalakis, Phys. Rev. B **73**, 233305 (2006).
[43]X. Hao, J. Li, C. Ding, P. Song, and X. Yang, Opt. Commun. **282**, 4276 (2009).
[44]Y. Qi, Y. Niu, Y. Xiang, H. Wang, and S. Gong, Opt. Commun. **284**, 276 (2011).
[45]Y. Xue, X. M. Su, G. Wang, Y. Chen, and J. Y. Gao, Opt. Commun. **249**, 231 (2005).
[46]S.-s. Ke and G.-x. Li, J. Phys.: Condens. Matter **20**, 175224 (2008).
[47]S. H. Asadpour, M. Jaberi, and H. R. Soleimani, J. Opt. Soc. Am. B **30**, 1815 (2013).